

Neuroimaging of dementia in 2013: what radiologists need to know

Sven Haller · Valentina Garibotto · Enikő Kövari ·
Constantin Bouras · Aikaterini Xekardaki ·
Cristelle Rodriguez · Maciej Jakub Lazarczyk ·
Panteleimon Giannakopoulos · Karl-Olof Lovblad

Received: 26 April 2013 / Revised: 29 May 2013 / Accepted: 10 June 2013 / Published online: 10 July 2013
© European Society of Radiology 2013

Abstract The structural and functional neuroimaging of dementia have substantially evolved over the last few years. The most common forms of dementia, Alzheimer disease (AD), Lewy body dementia (LBD) and fronto-temporal lobar degeneration (FTLD), have distinct patterns of cortical atrophy and hypometabolism that evolve over time, as reviewed in the first part of this article. The second part discusses unspecific white matter alterations on T2-weighted and fluid-attenuated inversion recovery (FLAIR) images as well as cerebral microbleeds, which often occur during normal aging and may affect cognition. The third part summarises molecular neuroimaging biomarkers recently developed to visualise amyloid deposits, tau protein deposits and neurotransmitter systems. The fourth section reviews the utility of advanced image analysis

techniques as predictive biomarkers of cognitive decline in individuals with early symptoms compatible with mild cognitive impairment (MCI). As only about half of MCI cases will progress to clinically overt dementia, whereas the other half remain stable or might even improve, the discrimination of stable versus progressive MCI is of paramount importance for both individual patient treatment and patient selection for clinical trials. The fifth and final part discusses the inter-individual variation in the neurocognitive reserve, which is a potential constraint for all proposed methods.

Key Points

- *Many forms of dementia have spatial atrophy patterns detectable on neuroimaging.*
- *Early treatment of dementia is beneficial, indicating the need for early diagnosis.*
- *Advanced image analysis techniques detect subtle anomalies invisible on radiological evaluation.*
- *Inter-individual variation explains variable cognitive impairment despite the same degree of atrophy.*

Keywords Dementia · Alzheimer · MCI · Cognitive decline · Frontal dementia · Fronto-temporal lobar degeneration

S. Haller · K.-O. Lovblad
Department of Imaging and Medical Informatics,
University Hospitals of Geneva and Faculty of Medicine
of the University of Geneva, Geneva, Switzerland

V. Garibotto
Department of Nuclear Medicine, Hospitals of Geneva and Faculty
of Medicine of the University of Geneva, Geneva, Switzerland

E. Kövari · C. Bouras · A. Xekardaki · C. Rodriguez ·
M. J. Lazarczyk · P. Giannakopoulos
Department of Mental Health and Psychiatry, University Hospitals
of Geneva and Faculty of Medicine of the University of Geneva,
Geneva, Switzerland

S. Haller (✉)
Service neuro-diagnostique et neuro-interventionnel DISIM,
University Hospitals of Geneva, Rue Gabrielle Perret-Gentil 4,
1211 Geneva 14, Switzerland
e-mail: sven.haller@me.com

Abbreviations

AD	Alzheimer disease
CAA	cerebral amyloid angiopathy
CBD	cortico-basal degeneration
CBS	cortico-basal syndrome
CMB	cerebral microbleeds
CMH	cerebral microhaemorrhages
DAI	diffuse axonal injury
CBD	corticobasal degeneration

DLB	dementia with Lewy bodies
DTI	diffusion tensor imaging
FDG	18F-fluorodeoxyglucose
FLAIR	fluid-attenuated inversion recovery
FTD	fronto-temporal dementia
FTLD	fronto-temporal lobar degeneration
GM	grey matter
GRE	gradient-echo
LPA	logopaenic aphasia
MCI	mild cognitive impairment
NBIA	neurodegeneration with brain iron accumulation
PCA	posterior cortical atrophy
PiB	¹¹ C-Pittsburgh compound B
PiD	Pick's disease
PET	positron emission tomography
PNFA	progressive non-fluent aphasia
PPA	primary progressive aphasia
PSP	progressive supranuclear palsy
SD	semantic dementia
SPECT	single photon emission computed tomography
SVM	support vector machine
SWI	susceptibility-weighted imaging
TBSS	tract-based spatial statistics
UBO	unspecific bright object
VaD	vascular dementia
VBM	voxel-based analysis
WM	white matter

Introduction

This review deals with the current state of neuroimaging of neurodegenerative diseases, especially dementias, seen from a radiologist's perspective. Initially it will review the basic radiological findings in dementias including specific patterns of atrophy, "unspecific" T2/FLAIR lesions and microbleeds. It will provide, as a comparison, the main findings of molecular imaging using nuclear medicine methods, i.e. positron emission tomography (PET) and single photon emission computed tomography (SPECT). It will provide an outlook for molecular biomarkers able to visualise amyloid deposits, tau protein deposits, various neurotransmitter systems and neuroinflammatory phenomena and a discussion of advanced image analysis tools, which are or will probably become available for clinical assessment in the near future. Then, this review will discuss an advanced image analysis tool able to detect subtle morphometric alterations that remain visible to the human eye. Finally, the inter-individual variation of the neurocognitive reserve will be reviewed, which potentially interferes with all the neuroimaging techniques discussed.

The complex and evolving concept of progressive neurodegeneration including the preclinical phase, especially Alzheimer disease (AD) (e.g. the review article by Lazarczyk

et al. [1]), goes beyond the scope of this review article, which is intended as a practical guide for radiologists.

Patterns of focal atrophy in common forms of dementia

The main objective of neuroimaging in dementia has been and remains the exclusion of other causes of dementia, especially treatable ones, such as normal pressure hydrocephalus, subdural haematomas or neoplasms including meningioma. Nevertheless, many (but not all) common forms of dementia are associated with typical patterns of focal atrophy, which will be discussed in the following section. Radiologists should be aware of these patterns in order to contribute to a specific diagnosis of dementia.

Alzheimer disease

Alzheimer disease (AD) is the most common form of dementia accounting for approximately 60–70 % (www.mghradrounds.org). The typical pattern of atrophy consists of atrophy of the hippocampus with consequent dilatation of the temporal horns of the lateral ventricles, associated with biparietal atrophy (as illustrated in Fig. 1). 18F-Fluorodeoxyglucose positron emission tomography (FDG-PET) typically shows a reduced glucose metabolism mainly in the posterior cingulate and precuneus and in the parieto-temporal regions (Fig. 1), probably owing to a combination of atrophy and hippocampal–neocortical disconnection phenomena [2]. These changes may appear early in the disease course, even in patients with a diagnosis of mild cognitive impairment (MCI) and earlier than hippocampal atrophy on morphological imaging.

Posterior cortical atrophy

Posterior cortical atrophy (PCA) is a rare type of dementia characterised by rapid and relatively selective decline in vision while memory and language skills are relatively preserved. PCA is considered by most authors as a variant of AD, with a characteristic atrophy and hypometabolism of the occipital lobe, which is often asymmetric (as illustrated in Fig. 2).

Dementia with Lewy bodies

Dementia with Lewy bodies (DLB) is the second most common type of dementia 25 % (www.mghradrounds.org). However, as there is no accepted specific pattern of atrophy (at least for visual inspection), radiologists cannot contribute to the diagnosis. As a consequence, radiologists may underestimate the high prevalence of this type of dementia. Molecular imaging, however, plays a key role in supporting the clinical diagnosis of DLB. FDG-PET shows a typical pattern of hypometabolism, which involves the occipital cortex and

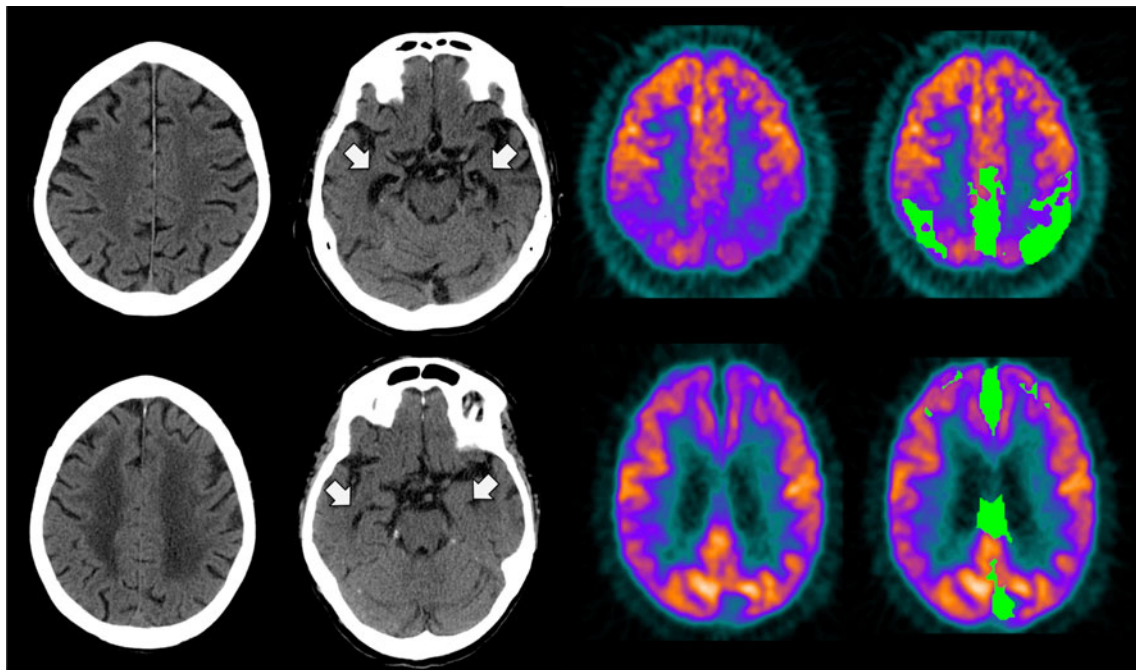


Fig. 1 Typical examples of Alzheimer disease (AD) (*top*) and vascular dementia (VaD) (*bottom*). Typical non-enhanced axial CT of an AD patient with focal atrophy of the hippocampus leading to dilation of the temporal horns of the lateral ventricles (*arrows*) and subtle biparietal atrophy. FDG-PET images show the typical hypometabolism of the posterior cingulate gyrus/precuneus and of the parietal and temporal cortex, bilaterally. These changes are visible on radioactivity distribution

images and are significant in comparison with a normal database using BRASS® software (see Sect. “Advanced image analyses” for details). Typical example of VaD with confluent signal alterations of the white matter. Note that in contrast to the AD patient (Fig. 1) of the same age, there is no focal atrophy of the peri-hippocampal region. FDG-PET images usually show preserved uptake in the posterior cingulate gyrus and focal hypometabolism, corresponding to vascular lesions

typically spares the metabolism of the posterior cingulate cortex (“cingulate island sign”), as shown in Fig. 3 [3]. Additionally the imaging of dopamine transporters, usually performed using SPECT and ¹²³I-ioflupane, shows that the nigro-striatal pathway is affected. This diagnostic test has a high sensitivity and specificity for the differential diagnosis of DLB vs. non-DLB dementias such as AD or vascular dementia (VaD): in the latter, the density of dopamine transporters is not reduced and ¹²³I-ioflupane uptake is preserved [4]. The normal distribution of ¹²³I-ioflupane is a “comma”-shaped uptake in the basal ganglia, whereas the pathologically reduced uptake in the putamen, with activity confined to the

head of the caudate nucleus, results in a “punctuation”-shaped uptake (Fig. 3).

Vascular dementia

Vascular dementia (VaD) is almost as prevalent as DLB (20 %, www.mghradrounds.org). VaD is characterised by confluent signal alterations of the white matter (WM) visible either as hypodensities on CT (as illustrated in Fig. 1) or hyperintense signal on T2/FLAIR MRI. In clinical routine, most patients have a combination of neurodegenerative dementia, e.g. AD, and a vascular component, as vascular changes are very

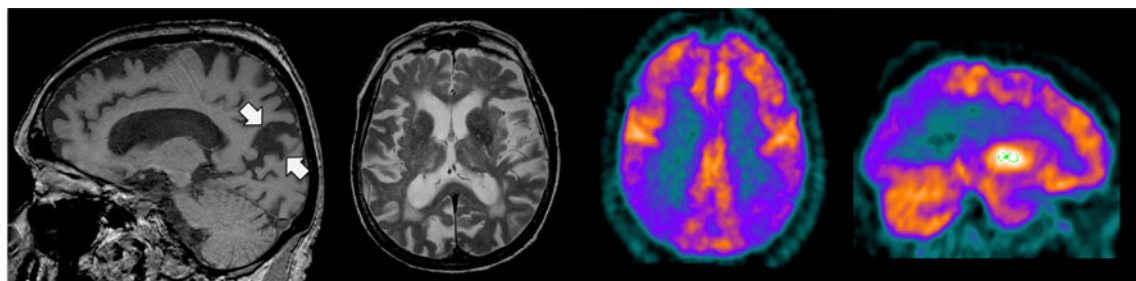
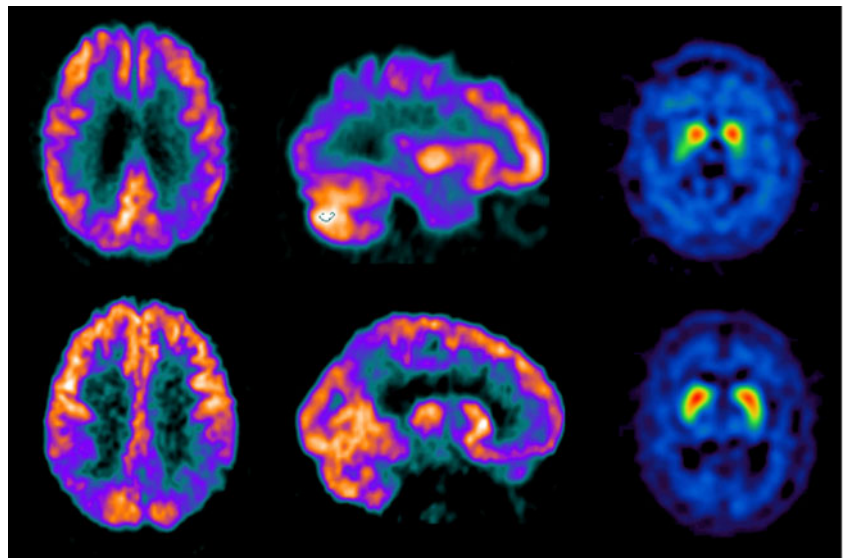


Fig. 2 Typical focal atrophy of the occipital lobe, which is often asymmetric, as in this case, and more pronounced on the right hemisphere. Note also the concomitant white matter abnormalities. FDG-PET

metabolism shows the hypometabolism of the occipital cortex in addition to the involvement of posterior cingulate and temporo-parietal cortices in patients with posterior cortical atrophy (PCA)

Fig. 3 Typical findings in dementia with Lewy bodies (DLB): hypometabolism of the parieto-occipital cortex with sparing of the posterior cingulate cortex, and reduced uptake of the ^{123}I -ioflupane in the basal ganglia. As a comparison, findings in AD are shown: a pattern of posterior hypometabolism sparing the occipital cortex and normal ^{123}I -ioflupane SPECT imaging



common during aging. Having a neurodegenerative disease is obviously not protective against concomitant vascular disease.

Fronto-temporal lobar degeneration

Fronto-temporal lobar degeneration is a heterogeneous group of dementias. Moreover, terminology and classification have changed over the last few years and different classifications exist. For the purpose of this review, and in order to avoid

misunderstandings, the term fronto-temporal lobar degeneration (FTLD) will be used for the entire group of dementias. Note that some authors use fronto-temporal dementia (FTD) as a term for the entire group, whereas others use this term as a subgroup of dementias including Pick's disease (PiD). To avoid misunderstandings, some authors use the term behavioural variant FTD (bvFTD) to unambiguously refer to the subgroup of dementias. Other subgroups of FTLD are progressive non-fluent aphasia (PNFA) and semantic dementia (SD). Some

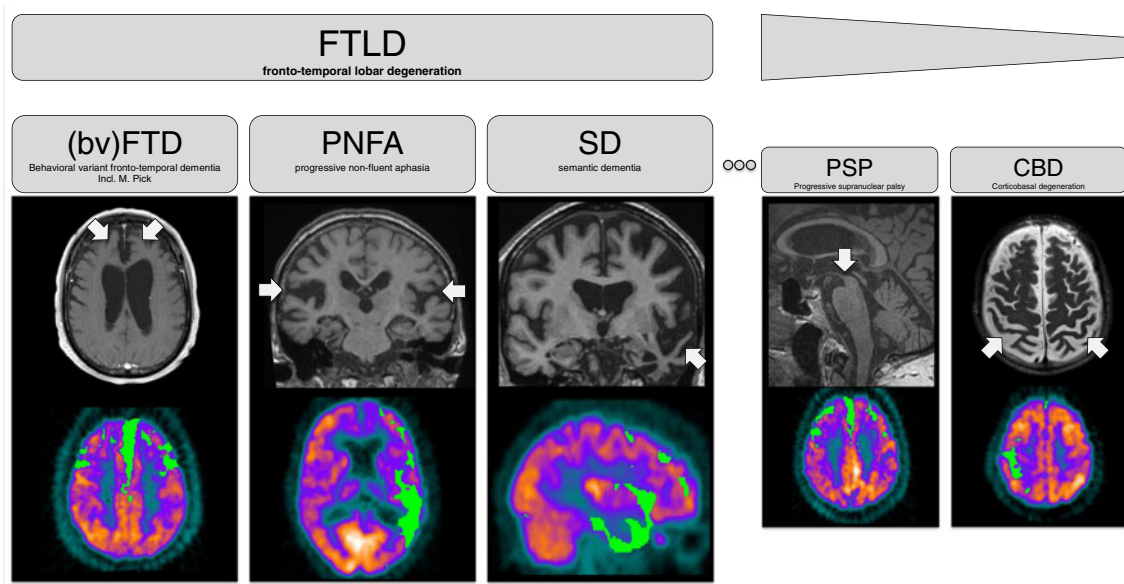


Fig. 4 Overview of dementias of the fronto-temporal lobar degeneration (FTLD) group. Behavioural FTD has frontal atrophy and hypometabolism with an anterior to posterior gradient. Progressive non-fluent aphasia (PNFA) often has bilateral peri-insular atrophy and left fronto-temporal hypometabolism. Semantic dementia (SD) has temporo-polar atrophy and hypometabolism with an anterior to posterior gradient, often more pronounced in the left hemisphere. Progressive supranuclear palsy syndrome (PSPS) and cortico-basal syndrome (CBS) are sometimes considered to be

additional types of FTLD. Progressive supranuclear palsy (PSP) may have additional neurocognitive decline and has typical midbrain atrophy leading to the penguin or hummingbird sign, whereas FDG-PET images also show cortical frontal hypometabolism. Cortico-basal degeneration (CBD) has bilateral parietal and sometimes associated infratentorial atrophy and typically asymmetric FDG-PET hypometabolism in fronto-parietal regions and possibly in subcortical regions

authors additionally consider progressive supranuclear palsy syndrome (PSPS) and cortico-basal syndrome (CBS) in the group of FTLD, both primarily neurodegenerative motor diseases yet sometimes with associated dementia, which can occasionally be the leading symptom [5] (Fig. 4).

bvFTD has characteristic atrophy and hypometabolism visible on FDG-PET images in both the frontal and anterior temporal lobes, with a characteristic anterior to posterior gradient. Note that images are acquired in the supine position. The brain is heavier than the cerebrospinal fluid and consequently in a declining occipital position. The occipital lobe is “squeezed” against the occipital bone, whereas the frontal lobe is floating in the cerebrospinal fluid and seems to open up. Therefore, neuroimaging typically overestimates frontal atrophy yet underestimates occipital atrophy.

PNFA typically has a bilateral peri-insular atrophy, and asymmetric left frontal and temporal hypometabolism.

SD is characterised by anterior temporo-polar atrophy and hypometabolism usually more pronounced on the left hemisphere, although right-dominant forms also exist.

Progressive non-fluent aphasia and semantic dementia are sometimes collectively called primary progressive aphasia (PPA). Logopaenic aphasia (LPA) has recently been described as a third subtype of PPA characterised by impaired word retrieval and sentence repetition yet intact motor speech and grammar [6, 7]. The atrophy typically predominates in left inferior frontal and posterior temporal regions [8]. Note that although LPA is considered a third variant of PPA, it is probably a variant of AD as opposed to the FTLD variants PNFA and SD. This is also supported by the finding of left parietal and posterolateral temporal lobe hypometabolism and positivity to amyloid PET imaging in these patients [9]. This rare form of dementia is not discussed in further detail in this review.

Although a detailed anatomical cortical measurement might reasonably well discriminate the main subtypes of FTLD [10], the imaging appearance of these forms of dementia, i.e. bvFTD, PNFA and SD, are variable, with considerable overlap [5]. A radiologist should thus detect if the atrophy of a given patient has a focal predominance in the frontal and laterotemporal regions with an anterior to posterior gradient and open the differential diagnosis of FTLD without insisting on a specific subgroup diagnosis.

PSP is primarily a neurodegenerative movement disorder characterised by a pattern of atrophy notably of the midbrain leading to the penguin or hummingbird sign [11], which can be quantified using for example the MR parkinsonism index [12]. A subgroup of PSP patients develop neurocognitive decline and in some cases the cognitive impairment may even be the leading symptom. FDG-PET images show a typical cortical hypometabolism in the whole prefrontal cortex, associated with hypometabolism in the basal ganglia, thalamus and mesencephalon.

CBD is, similar to PSP discussed above, primarily a neurodegenerative movement disorder involving cortico-basal degeneration, yet a subgroup of patients develop neurocognitive decline. In analogy to PSP discussed above, the cognitive impairment may be the leading symptom in some cases. CBS typically has a focal biparietal atrophy. Unlike AD, biparietal focal atrophy is not associated with peri-hippocampal atrophy but sometimes with infratentorial cerebellar atrophy. FDG-PET images typically show a unilateral or strongly asymmetric cortical (parietal, prefrontal and motor cortex) and subcortical hypometabolism, contralateral to the affected body side.

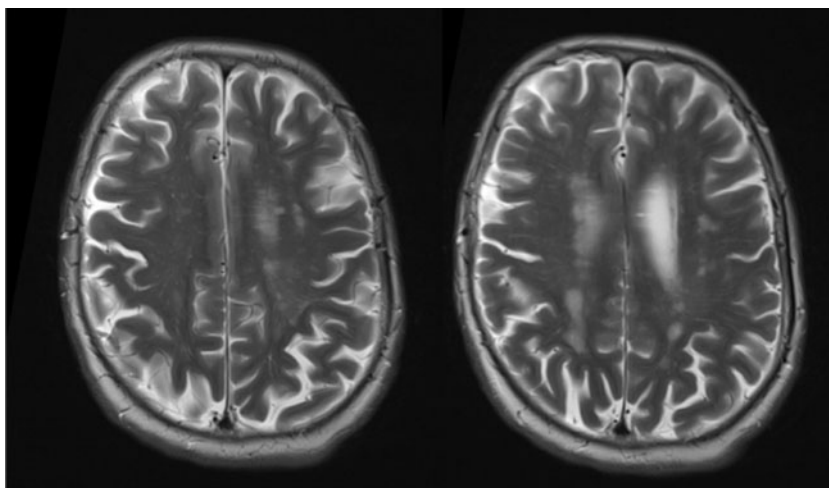
Neurodegeneration with brain iron accumulation

Neurodegeneration with brain iron accumulation (NBIA) is a rare group of diseases with an estimated incidence of 1–3/1,000,000 characterised by brain iron accumulation notably in the basal ganglia. Pantothenate kinase-associated neurodegeneration (PKAN), formally known as Hallervorden–Spatz syndrome, is the most widely known disease of this group. It is caused by a mutation of the *PANK-2* gene (pantothenate kinase) at chromosome 20p13. Other forms include infantile neuroaxonal dystrophy (INAD), neuroferritinopathy, aceruloplasminaemia, Kufor-Rakeb disease (KRD), fatty acid hydroxylase-related neurodegeneration (FAHN) as well as a group of idiopathic NBIA of (still) unknown origin. These conditions show a wide clinical and pathological spectrum including spastic paraplegias, leukodystrophies and neuronal ceroid lipofuscinosis. Imaging appearance is also variable. The typical imaging sign called the “eye of the tiger” consists of a central hyperintensity of the globus pallidus with surrounding hypointensity on T2w images, and can be identified in most cases of PKAN [13]. Although NBIA in most cases is a disease of infants and children with extrapyramidal movement disorders, adult forms of NBIA exist and sometimes dementia may be the leading symptom. Therefore this condition, even though generally a rare cause of dementia, is briefly mentioned in this review.

“Non-specific” white matter T2/FLAIR lesions and normal aging

Hyperintense signal alterations of the WM on T2 and FLAIR images are very common findings in the elderly (a typical example is illustrated in Fig. 5). These “unspecific” WM lesions, sometimes also called unspecific bright objects (UBOs), have a prevalence of about 15 % at the age of 60, and around 80 % at the age of 80 [14–16]. Generally speaking, these “unspecific” WM lesions are associated with an increased risk of cognitive decline and dementia, stroke and even death [16, 17]. When looking at the correlation between T2w lesions and neurocognitive decline in more detail, however, it becomes more controversial. For example, only five out of eight studies

Fig. 5 A typical example of “unspecific” white matter signal alterations during normal aging



found an association between WM hyperintensities and global cognitive decline, whereas the remaining three studies were negative [16]. This might be attributed to the inter-individual variation of the cognitive reserve (discussed in detail in Sect. “Neurocognitive reserve mechanisms and imaging biomarkers”) [18]. The correlation between radiological WM lesions and histopathology is no less controversial. Despite the very frequent observation of WM hyperintensities on MRI, radiological–pathological correlation studies, especially in combination with pre-mortem MRI, are rare [19]. Histopathological correlates of T2w hyperintensities are very heterogeneous [20] and include myelin pallor, tissue rarefaction including loss of myelin and axons as well as mild gliosis [16, 21–24]. A recent investigation [25] correlated pre-mortem WM hyperintensities with post-mortem MRI in 59 healthy elderly persons and found that MRI overestimates periventricular

lesions yet underestimates deep WM lesions with respect to histopathological demyelination. This might be due to the relatively high local water content in the periventricular lesions in combination with increasing blood–brain barrier permeability which occurs during aging [26] and which tends to cause T2 and FLAIR hyperintense signal on MRI compared with the deep WM which has a relatively lower local water content. Correspondingly, whereas most correlation studies assess global WM lesion load, some studies separately assessed periventricular and deep WM lesions and indicate higher clinical relevance of deep versus periventricular T2-weighted hyperintensities [15, 27]. Future correlation studies are necessary, ideally combining multiple imaging contrasts including T2/FLAIR, diffusion tensor imaging (DTI) and magnetisation transfer, in order to better describe and understand the histopathological correlates of WM lesions detected on MRI.

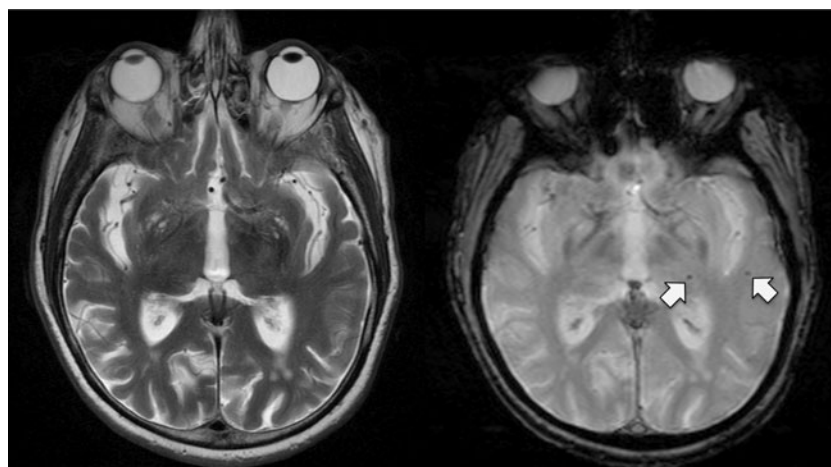


Fig. 6 Example of typical microbleeds in the context of a hypertensive microvascular leucoencephalopathy. Microbleeds are small hypointense signal alterations on gradient-echo T2*w imaging (*right*), which are (usually not) visible on standard spin-echo T2w (*left*). The random

distribution of the microbleeds including the basal ganglia, the clinical context of arterial hypertension and the diffuse white matter T2w hyperintensities (microvascular leucoencephalopathy, not illustrated) suggests the diagnosis of hypertensive cerebral microbleeds

Cerebral microbleeds

Cerebral microbleeds (CMB) or cerebral microhaemorrhages (CMH) are small hypointense lesions seen on susceptibility imaging with variable cut-off size in the literature typically between 5 and 10 mm [28–31] (see Fig. 6 for an example of hypertensive microbleeds). CMBs have attracted growing interest in recent years. This may at least partly be explained by the wide availability of high-field MRI systems and novel imaging sequences, in particular susceptibility-weighted imaging (SWI), as these technical developments increase the number of detectable microbleeds [32]. For example, SWI identified significantly more CMBs than T2* in 141 patients in a memory clinic setting [29]. This increase in detection rate of 40 % in SWI versus 23 % in T2* did, however, not improve the correlation with vascular risk factors or radiological markers of small-vessel disease.

Similar to the WM hyperintensities discussed above, clinical–radiological correlation studies of CMBs are rare and often produce partially conflicting data [33–35]. The prevalence of microhaemorrhages is higher in VaD (65 %) than in MCI (20 %) or AD (18 %) using T2*w imaging [30]. An SWI study at 3 T principally replicated these results [36] as follows: VaD (86 %), DLB (54 %), AD (48 %), MCI (41 %) and clearly less commonly in FTLN (27 %) and subjective cognitive complaints (22 %). SWI detected more microhaemorrhages than T2*, as expected from previous studies cited above. Although the number of CMBs is increased in MCI, it is less clear whether CMB load may predict further cognitive decline. Whereas the frequency of CMBs at baseline did not differ between controls and MCI (11 % and 14 % respectively), cases with more than three microhaemorrhages were found only within the progressive MCI group [33]. Another study found that only one of 23 stable MCI but 8 of 26 progressive MCI had more than one CMH at baseline [34]. Yet another study found a higher rate of CMBs in MCI (0.6 ± 0.9) than in controls (0.2 ± 0.5), yet the number of microhaemorrhages did not discriminate stable versus progressive MCI. In summary, these findings indicate a detrimental effect of CMBs [37].

Concerning the radiological–histopathological correlation of CMB, available data are also rare, again similar to the WM hyperintensities discussed above. The prevalence of CMBs on histopathology is around 60–70 % in the age group above 80–85 years [38, 39]. The radiological studies discussed above reported lower rates of CMBs on imaging (although admittedly the age was a little lower in some studies), indicating that neuroimaging may have some false-negative results. The few available radiological–histopathological correlation studies of CMBs also demonstrate false-positive results of neuroimaging. For example, one T2* study found true-positive radiological–histopathological correlation in 21 of 34 lesions (62 %), whereas haemosiderin deposits were noted without MR signal changes in two (of 11) brains (false negatives 18 %) [40].

Another more recent study assessed SWI CMBs in a preselected sample of dementia patients with cerebral amyloid angiopathy [41]. Of the 38 SWI CMBs, the authors identified 7 small cavities, 1 dissection in the wall of a grossly distended vessel and 1 microaneurysm ($7+1+1=24$ % false negatives). The authors concluded that “...the underlying pathologic lesions we discovered correlating to (MRI) hypointensities were quite varied” [41]. In conclusion, CMB “mimics” include micro-dissection, microaneurysm, microcalcifications and arteriolar pseudocalcification [40–42].

The most important differential diagnoses of multiple microbleeds include cerebral amyloid angiopathy (CAA), multiple (micro-)cavernomas and haemorrhagic diffuse axonal injury (DAI), which will be only very briefly discussed in the context of the current review on dementias. CAA is characterised by multiple microbleeds typically at the grey–white matter junction in a parieto-occipital lobar distribution sparing the basal ganglia and infratentorial regions. Multiple familial (micro-)cavernomas can usually be identified, as at least one cavernoma is large enough to create the typical “pop-corn” image on T2w imaging. Radiation-induced multiple micro-cavernomas can be identified on the basis of the patient’s history. Finally, traumatic haemorrhagic DAI can again be identified on the basis of the clinical context and eventually other traumatic lesions such as fractures or subdural haematomas.

Today, there are no generally accepted guidelines concerning the interpretation of CBMs, for example how many CMBs are considered normal for a given age group, or whether some locations of CMBs might be clinically more relevant than other locations. Again, in agreement with the WM hyperintensities discussed above, future correlative studies are needed to improve our understanding of the diagnosis and nature of small regions of signal loss on T2* and SWI sequences.

Nuclear medicine: molecular imaging

The marker most commonly used is PET imaging of brain metabolism, using FDG as a tracer. This technique shows typical hypometabolic patterns in different dementia syndromes, as shown in Figs. 1, 2, 3 and 4, with an overall superior sensitivity than hypoperfusion assessment by SPECT [43]. A second molecular marker used for the differential diagnosis of dementias is dopamine transporter imaging, mainly by SPECT and ^{123}I -ioflupane (see Fig. 3).

Over the last decade, specific nuclear medicine tracers able to visualise *in vivo* amyloid plaques, which represent an important pathological hallmark of AD, have been tested and validated in humans. Most amyloid imaging investigations published to date have used ^{11}C -Pittsburgh compound B (PiB) as a tracer [44]. This tracer has been proven to be able to bind fibrillary amyloid with a good correlation with post-

mortem measures [45]. Newer ^{18}F -labeled compounds, which have been recently patented, are also becoming available, and will presumably have a wider diffusion in clinical practice, owing to their greater availability. This is linked to the longer half-life of the isotope: whereas ^{11}C has a half-life of 20 min, needing an onsite cyclotron for production of the tracer, ^{18}F has a half-life of 110 min and therefore the tracer can be produced off-site.

In recent years, many studies have investigated the use of amyloid imaging markers. Excellent correspondence was demonstrated between ante-mortem amyloid PET imaging findings and $\text{A}\beta$ deposition in the brain at autopsy [46]. A consistent finding across different studies is that around 30 % of cognitively normal elderly subjects have abnormal findings on PET amyloid imaging studies, which matches quite well the proportion of cognitively normal elderly subjects with an autopsy diagnosis of AD [47, 48]. These individuals are presumably at risk of subsequently developing dementia, a risk possibly modulated by their neurocognitive reserve potential. A recent multicentre European study on amyloid PET imaging in MCI and AD has shown that none of the MCI amyloid-negative patients converted to AD, indicating that this imaging method has an excellent negative predictive value for progression to AD [49]. These tracers will mainly be used for confirming a diagnosis of AD when clinically suspected, for early diagnosis in MCI subjects, and for differential diagnosis with other forms of amyloid-negative dementia, such as FLTD [50].

Specific tracers also exist that are able to visualise both amyloid and tau aggregates, which are the other major histopathological hallmarks of AD [51], or tau aggregates alone [52], but clinical experience with these tracers is still quite limited.

Molecular imaging by radioactive tracers also allows other phenomena to be explored, such as neuroinflammation, which occurs in some forms of dementia [53, 54], or specific neurotransmission systems, such as the cholinergic [55, 56], serotonergic [57] and the previously mentioned dopaminergic system, among others. The discussion of these applications, which are still limited to research settings for the moment, goes beyond the scope of this review.

Advanced image analyses

Although there are currently no generally accepted disease-modifying treatments for AD, several promising candidates are currently being evaluated (for review, see Nitsch and Hock [58] and Duara et al. [59]). Early treatment is probably more beneficial in stopping or at least slowing down the progressive neurodegeneration than treatment of clinically overt dementia at a late stage [60, 61]. This implies the need for early diagnosis parameters including neuroimaging, and explains the interest in MCI, which was initially perceived as a prodromal state of AD [62]. The concept of MCI has evolved in recent years and now

represents a heterogeneous group of various subtypes of MCI, with different progression rates of the various MCI subtypes [62–65].

Note that without further preselection, only about half of MCI subjects will progress to AD, whereas the other half remain stable or may even improve. This is problematic for early treatment of MCI individuals (half of MCI individuals may be treated despite the fact that they would remain stable even without treatment) as well as for clinical trials. For a typical placebo-controlled trial, 50 % of MCI patients remain stable even without treatment. Only 25 % of cases are progressive MCI and obtain the active medication. On the other hand, 25 % of cases are stable MCI and remain stable despite being in the placebo group. This explains why it is extremely difficult to demonstrate a beneficial drug-related effect in unselected MCI cases.

This need for early detection of at-risk patients led to the creation of the Alzheimer Disease Neuroimaging Initiative (ADNI) [66], the first large multicentre study with standardised MR imaging parameters, also including additional neurocognitive and other (serology etc.) assessments. The data are shared via the Internet with research groups all over the world, and this has led to multiple publications that have significantly improved the understanding of the progression of neurodegeneration as well as new image analysis tools, amongst others. This project also led to several currently on-going offspring studies, such as its European equivalent AddNeuroMed [67]. The ADNI project has led to a standardisation of MR imaging parameters, and many centres today use the ADNI imaging parameters even for clinical assessment of patients not enrolled in studies.

Advanced image analysis techniques concerning this topic are based on the assumption that subtle and systematic changes in brain structure already exist during the early phase of neurodegeneration, yet these changes are too subtle to be detected by standard visual inspection of the MRI and are detectable only by advanced image analysis techniques such as voxel-based morphometric (VBM) analysis of grey matter (GM) [68], e.g. in MCI [69–74], or DTI-based analysis of WM, e.g. implementing voxel-wise tract-based spatial statistical analysis (TBSS) [75], e.g. in MCI [76–84]. Most of these advanced image analysis studies used group-level comparisons, comparing typically patients with MCI versus controls and/or AD. Although such studies detect the spatial distribution of structural brain alterations during neurodegeneration, these group-level results cannot be transferred to the detection of individual patients in a clinical context. This has led to a fundamental shift in the paradigm and the application of classification analyses. The basic principle of such classification analyses can be explained with the example of face recognition. Although on average, two groups of persons might have the most pronounced group-level differences for example at the tip of the nose, it is not possible to detect an individual face only using this single parameter (“feature” in the terminology

of classification analyses). On the other hand, individual faces can be recognised by a specific pattern, which combines multiple features (such as ears, lips, eyes etc.) although each feature per se is not necessarily significantly different between groups (see Haller et al. for a review [85]). Support vector machines (SVM) [86] are a currently frequently implemented technique as the specific properties of this classification technique are well adapted to neuroimaging data. Note, however, that multiple other classification techniques exist and that the field is rapidly evolving, indicating that other classifiers may provide better or more robust results and replace the currently most commonly implemented SVM classifier in the future. The discrimination between stable versus progressive MCI based on SVM classifiers was possible with an accuracy of 85–90 % using GM [87–89], 90–95 % using WM DTI [83, 84] and 85 % using iron deposition SWI [35]. Moreover it is possible to classify the different MCI subtypes with very high accuracy [90]. Assuming that different MCI subtypes best respond to different treatment options, this MCI subtype classification may be relevant in order to ascertain the optimal treatment at an individual level.

Current projects aim to combine multiple imaging techniques (sometimes with other parameters such as cerebrospinal fluid analysis, electroencephalography etc.) with the aim of further improving the classification accuracy and in particular the robustness of classification of for example MRI data acquired on different MRI machines at different field strengths. Although the concept of combining multiple imaging techniques is evident and straightforward, the technical implementation and in particular optimising the combination of multiple classification parameters are much more challenging [85]. One example is a recent study demonstrating that the combination of DTI-derived structural connectivity and resting-state fMRI-derived functional connectivity did indeed improve classification accuracy [91].

As many patients undergo MR imaging for clinical reasons, notably to exclude other diseases, these advanced image analysis techniques in principle reuse existing MRI data as long as standard imaging protocols are adopted. In order to be clinically useable in daily routine practice, these classification methods must be optimised and adapted to routine clinical neuroradiological use. Current developments include software installations directly implemented on the MRI machine or cloud-based solutions evaluating individual cases uploaded via the Internet to provide automated evaluation of individual patients. Currently, these solutions still require technical improvements and validation for medico-legal approval before they can be used in clinical routine.

For FDG-PET techniques the region-wise or voxel-wise comparison of individual PET images, normalised to the global uptake or to the uptake in a preserved region (often the cerebellum is chosen for this purpose) with a database of PET images acquired in healthy, ideally age-matched, individuals,

is an important advance in image analysis, which already plays a relevant role in clinical practice. Such analyses provide maps of significant deviations from the normal population. The examples provided in Figs. 1 and 4 show the added value of this analysis: it clearly depicts patterns of reduced metabolism and limits subjectivity in image interpretation. Various research and commercial software tools are available for this purpose, providing complementary approaches to this problem (region-based analyses, automated classification, etc.) and have been tested in numerous clinical studies [92–96].

Neurocognitive reserve mechanisms and imaging biomarkers

Owing to individual predisposition, education, social context and other factors, some individuals may maintain normal cognitive functions longer than other individuals despite a similar degree of neurodegeneration—or from the other perspective, the same amount of neurodegeneration may lead to a variable degree of clinical cognitive decline, as first described in 1968 [97]. Various neuroimaging studies have documented a reserve phenomenon in dementias, mainly in AD, but also in other dementia types such as FTD or DLB, showing an association between education, occupation, socioeconomic status and measures of an on-going neuropathological process, such as brain atrophy, reduced brain perfusion and metabolism, or increased amyloid deposition, when correcting for clinical and neuropsychological severity [98–103]. These observations may explain the sometimes poor correlation between neuroimaging biomarkers and cognitive function and should be taken into account when interpreting such biomarkers as a potential constraint for all advanced analysis techniques.

Conclusions

The radiologist needs to be aware that many forms of dementia have typical patterns of focal brain atrophy. Attentive visual inspection of focal atrophy may sometimes contribute to the diagnosis of a specific form of dementia, leading neuroimaging beyond the pure exclusion of other diseases. Nevertheless, radiologists should be aware of the inter-individual variation in the neurocognitive reserve, meaning that the same amount of brain pathological features will lead to a variable degree of cognitive symptoms depending on individual factors, education, social integration etc. Standardised imaging protocols using both “standard imaging techniques” and advanced sequences or molecular imaging together with multiple new advanced data analyses are currently being evaluated, and may in the near future contribute to the computer-aided early diagnosis of subtle brain structural changes at an individual patient level. Thus we may see what is at the moment still

“invisible” during primary radiological inspection. The radiologist should be able to contribute to an early diagnosis of cognitive decline that will help to select at-risk patients for clinical trials in order to improve patients’ outcomes.

Acknowledgments This work is supported by Swiss National Foundation grant SNF 3200B0-116193 and SPUM 33CM30-124111.

Editor’s note Readers will notice that this issue contains two rather similar review articles on the imaging of dementia. Both articles try to help the average radiologist identify key features which may require expert neuroradiological attention. Two groups spontaneously submitted a review article at roughly the same time. There were merits in both papers; both were favourably reviewed. It was an impossible editorial choice to select one paper over another and hence both are published alongside each other. It will be interesting to see whether the astute readers will identify differences. Indeed this may lead to some interesting discussion in the opinion column on the journal’s website.

Disclosure No conflicts of interest

References

- Lazarczyk MJ, Hof PR, Bouras C et al (2012) Preclinical Alzheimer disease: identification of cases at risk among cognitively intact older individuals. *BMC Med* 10:127
- Chetelat G, Desgranges B, Landeau B et al (2008) Direct voxel-based comparison between grey matter hypometabolism and atrophy in Alzheimer’s disease. *Brain* 131:60–71
- Lim SM, Katsifis A, Villemagne VL et al (2009) The 18F-FDG PET cingulate island sign and comparison to 123I-beta-CIT SPECT for diagnosis of dementia with Lewy bodies. *J Nucl Med* 50:1638–1645
- McKeith I, O’Brien J, Walker Z et al (2007) Sensitivity and specificity of dopamine transporter imaging with 123I-FP-CIT SPECT in dementia with Lewy bodies: a phase III, multicentre study. *Lancet Neurol* 6:305–313
- Rohrer JD (2012) Structural brain imaging in frontotemporal dementia. *Biochim Biophys Acta* 1822:325–332
- Gorno-Tempini ML, Dronkers NF, Rankin KP et al (2004) Cognition and anatomy in three variants of primary progressive aphasia. *Ann Neurol* 55:335–346
- Gorno-Tempini ML, Hillis AE, Weintraub S et al (2011) Classification of primary progressive aphasia and its variants. *Neurology* 76:1006–1014
- Rohrer JD, Ridgway GR, Crutch SJ et al (2010) Progressive logopenic/phonological aphasia: erosion of the language network. *NeuroImage* 49:984–993
- Rabinovici GD, Jagust WJ, Furst AJ et al (2008) Abeta amyloid and glucose metabolism in three variants of primary progressive aphasia. *Ann Neurol* 64:388–401
- Lindberg O, Ostberg P, Zandbelt BB et al (2009) Cortical morphometric subclassification of frontotemporal lobar degeneration. *AJNR Am J Neuroradiol* 30:1233–1239
- Groschel K, Kastrop A, Litvan I et al (2006) Penguins and hummingbirds: midbrain atrophy in progressive supranuclear palsy. *Neurology* 66:949–950
- Quattrone A, Nicoletti G, Messina D et al (2008) MR imaging index for differentiation of progressive supranuclear palsy from Parkinson disease and the Parkinson variant of multiple system atrophy. *Radiology* 246:214–221
- Hayflick SJ, Hartman M, Coryell J et al (2006) Brain MRI in neurodegeneration with brain iron accumulation with and without PANK2 mutations. *AJNR Am J Neuroradiol* 27:1230–1233
- Garde E, Mortensen EL, Krabbe K et al (2000) Relation between age-related decline in intelligence and cerebral white-matter hyperintensities in healthy octogenarians: a longitudinal study. *Lancet* 356:628–634
- Ylikoski A, Erkinjuntti T, Raininko R et al (1995) White matter hyperintensities on MRI in the neurologically nondiseased elderly. Analysis of cohorts of consecutive subjects aged 55 to 85 years living at home. *Stroke* 26:1171–1177
- Debette S, Markus HS (2010) The clinical importance of white matter hyperintensities on brain magnetic resonance imaging: systematic review and meta-analysis. *BMJ* 341:c3666
- Inzitari D, Simoni M, Pracucci G et al (2007) Risk of rapid global functional decline in elderly patients with severe cerebral age-related white matter changes: the LADIS study. *Arch Intern Med* 167:81–88
- Murray AD, Staff RT, McNeil CJ et al (2011) The balance between cognitive reserve and brain imaging biomarkers of cerebrovascular and Alzheimer’s diseases. *Brain* 134:3687–3696
- Young VG, Halliday GM, Kril JJ (2008) Neuropathologic correlates of white matter hyperintensities. *Neurology* 71:804–811
- Gouw AA, Seewann A, van der Flier WM et al (2011) Heterogeneity of small vessel disease: a systematic review of MRI and histopathology correlations. *J Neurol Neurosurg Psychiatry* 82:126–135
- Pantoni L, Garcia JH (1997) Pathogenesis of leukoaraiosis: a review. *Stroke* 28:652–659
- Fazekas F, Kleinert R, Offenbacher H et al (1993) Pathologic correlates of incidental MRI white matter signal hyperintensities. *Neurology* 43:1683–1689
- Grafton ST, Sumi SM, Stimac GK et al (1991) Comparison of postmortem magnetic resonance imaging and neuropathologic findings in the cerebral white matter. *Arch Neurol* 48:293–298
- van Swieten JC, van den Hout JH, van Ketel BA et al (1991) Periventricular lesions in the white matter on magnetic resonance imaging in the elderly. A morphometric correlation with arteriosclerosis and dilated perivascular spaces. *Brain* 114:761–774
- Haller S, Kovari E, Herrmann FR et al (2013) Do brain T2/FLAIR white matter hyperintensities correspond to myelin loss in normal aging? A radiologic-neuropathologic correlation study. *Acta Neuropathologica Commun* 1:14
- Topkian R, Barrick TR, Howe FA et al (2010) Blood-brain barrier permeability is increased in normal-appearing white matter in patients with lacunar stroke and leukoaraiosis. *J Neurol Neurosurg Psychiatry* 81:192–197
- de Groot JC, de Leeuw FE, Oudkerk M et al (2000) Cerebral white matter lesions and depressive symptoms in elderly adults. *Arch Gen Psychiatry* 57:1071–1076
- Greenberg SM, Vernooij MW, Cordonnier C et al (2009) Cerebral microbleeds: a guide to detection and interpretation. *Lancet Neurol* 8:165–174
- Goos JD, van der Flier WM, Knol DL et al (2011) Clinical relevance of improved microbleed detection by susceptibility-weighted magnetic resonance imaging. *Stroke* 42:1894–1900
- Cordonnier C, van der Flier WM, Sluimer JD et al (2006) Prevalence and severity of microbleeds in a memory clinic setting. *Neurology* 66:1356–1360
- Cordonnier C, Al-Shahi Salman R, Wardlaw J (2007) Spontaneous brain microbleeds: systematic review, subgroup analyses and standards for study design and reporting. *Brain* 130:1988–2003
- Nandigam RN, Viswanathan A, Delgado P et al (2009) MR imaging detection of cerebral microbleeds: effect of susceptibility-weighted imaging, section thickness, and field strength. *AJNR Am J Neuroradiol* 30:338–343

33. Ayaz M, Boikov AS, Haacke EM et al (2010) Imaging cerebral microbleeds using susceptibility weighted imaging: one step toward detecting vascular dementia. *J Magn Reson Imaging* 31:142–148
34. Kirsch W, McAuley G, Holshouser B et al (2009) Serial susceptibility weighted MRI measures brain iron and microbleeds in dementia. *J Alzheimers Dis* 17:599–609
35. Haller S, Bartsch A, Nguyen D et al (2010) Cerebral microhemorrhage and iron deposition in mild cognitive impairment: susceptibility-weighted MR imaging assessment. *Radiology* 257:764–773
36. Uetani H, Hirai T, Hashimoto M et al (2013) Prevalence and topography of small hypointense foci suggesting microbleeds on 3T susceptibility-weighted imaging in various types of dementia. *AJNR Am J Neuroradiol* 34:984–989
37. Gold G, Giannakopoulos P, Herrmann FR et al (2007) Identification of Alzheimer and vascular lesion thresholds for mixed dementia. *Brain* 130:2830–2836
38. Fisher M, French S, Ji P et al (2010) Cerebral microbleeds in the elderly: a pathological analysis. *Stroke* 41:2782–2785
39. Tanskanen M, Makela M, Myllykangas L et al (2012) Intracerebral hemorrhage in the oldest old: a population-based study (van-taa 85+). *Front Neurol* 3:103
40. Fazekas F, Kleinert R, Roob G et al (1999) Histopathologic analysis of foci of signal loss on gradient-echo T2*-weighted MR images in patients with spontaneous intracerebral hemorrhage: evidence of microangiopathy-related microbleeds. *AJNR Am J Neuroradiol* 20:637–642
41. Schrag M, McAuley G, Pomakian J et al (2010) Correlation of hypointensities in susceptibility-weighted images to tissue histology in dementia patients with cerebral amyloid angiopathy: a postmortem MRI study. *Acta Neuropathol* 119:291–302
42. Tatsumi S, Shinohara M, Yamamoto T (2008) Direct comparison of histology of microbleeds with postmortem MR images: a case report. *Cerebrovasc Dis* 26:142–146
43. Torosyan N, Silverman DH (2012) Neuronuclear imaging in the evaluation of dementia and mild decline in cognition. *Semin Nucl Med* 42:415–422
44. Klunk WE, Engler H, Nordberg A et al (2004) Imaging brain amyloid in Alzheimer's disease with Pittsburgh compound-B. *Ann Neurol* 55:306–319
45. Nordberg A (2011) Molecular imaging in Alzheimer's disease: new perspectives on biomarkers for early diagnosis and drug development. *Alzheimers Res Ther* 3:34
46. Clark CM, Schneider JA, Bedell BJ et al (2011) Use of florbetapir-PET for imaging beta-amyloid pathology. *JAMA* 305:275–283
47. Aizenstein HJ, Nebes RD, Saxton JA et al (2008) Frequent amyloid deposition without significant cognitive impairment among the elderly. *Arch Neurol* 65:1509–1517
48. Chetelat G, Villemagne VL, Pike KE et al (2011) Independent contribution of temporal beta-amyloid deposition to memory decline in the pre-dementia phase of Alzheimer's disease. *Brain* 134:798–807
49. Nordberg A, Carter SF, Rinne J et al (2013) A European multicentre PET study of fibrillar amyloid in Alzheimer's disease. *Eur J Nucl Med Mol Imaging* 40:104–114
50. Rowe CC, Ng S, Ackermann U et al (2007) Imaging beta-amyloid burden in aging and dementia. *Neurology* 68:1718–1725
51. Small GW, Kepe V, Ercoli LM et al (2006) PET of brain amyloid and tau in mild cognitive impairment. *N Engl J Med* 355:2652–2663
52. Fodero-Tavoletti MT, Okamura N, Furumoto S et al (2011) 18F-THK523: a novel in vivo tau imaging ligand for Alzheimer's disease. *Brain* 134:1089–1100
53. Cagnin A, Kassio M, Meikle SR et al (2006) In vivo evidence for microglial activation in neurodegenerative dementia. *Acta Neurol Scand Suppl* 185:107–114
54. Iannaccone S, Cerami C, Alessio M et al (2013) In vivo microglia activation in very early dementia with Lewy bodies, comparison with Parkinson's disease. *Parkinsonism Relat Disord* 19:47–52
55. Marcone A, Garibotto V, Moresco RM et al (2012) [(11)C]-MP4A PET cholinergic measurements in amnesic mild cognitive impairment, probable Alzheimer's disease, and dementia with Lewy bodies: a Bayesian method and voxel-based analysis. *J Alzheimers Dis* 31:387–399
56. Kendziorra K, Wolf H, Meyer PM et al (2011) Decreased cerebral alpha4beta2* nicotinic acetylcholine receptor availability in patients with mild cognitive impairment and Alzheimer's disease assessed with positron emission tomography. *Eur J Nucl Med Mol Imaging* 38:515–525
57. Franceschi M, Anchisi D, Pelati O et al (2005) Glucose metabolism and serotonin receptors in the frontotemporal lobe degeneration. *Ann Neurol* 57:216–225
58. Nitsch RM, Hock C (2008) Targeting beta-amyloid pathology in Alzheimer's disease with Abeta immunotherapy. *Neurotherapeutics* 5:415–420
59. Duara R, Barker W, Loewenstein D et al (2009) The basis for disease-modifying treatments for Alzheimer's disease: the sixth annual mild cognitive impairment symposium. *Alzheimers Dement* 5:66–74
60. Holmes C, Boche D, Wilkinson D et al (2008) Long-term effects of Abeta42 immunisation in Alzheimer's disease: follow-up of a randomised, placebo-controlled phase I trial. *Lancet* 372:216–223
61. Lannfelt L, Blennow K, Zetterberg H et al (2008) Safety, efficacy, and biomarker findings of PBT2 in targeting Abeta as a modifying therapy for Alzheimer's disease: a phase IIa, double-blind, randomised, placebo-controlled trial. *Lancet Neurol* 7:779–786
62. Petersen RC (2004) Mild cognitive impairment as a diagnostic entity. *J Intern Med* 256:183–194
63. Petersen RC, Negash S (2008) Mild cognitive impairment: an overview. *CNS Spectr* 13:45–53
64. Mariani E, Monastero R, Mecocci P (2007) Mild cognitive impairment: a systematic review. *J Alzheimers Dis* 12:23–35
65. Forlenta OV, Diniz BS, Nunes PV et al (2009) Diagnostic transitions in mild cognitive impairment subtypes. *Int Psychogeriatr* 21:1088–1095
66. Mueller SG, Weiner MW, Thal LJ et al (2005) Ways toward an early diagnosis in Alzheimer's disease: the Alzheimer's Disease Neuroimaging Initiative (ADNI). *Alzheimers Dement* 1:55–66
67. Lovestone S, Francis P, Kloszewska I et al (2009) AddNeuroMed—the European collaboration for the discovery of novel biomarkers for Alzheimer's disease. *Ann N Y Acad Sci* 1180:36–46
68. Ashburner J, Friston KJ (2000) Voxel-based morphometry—the methods. *NeuroImage* 11:805–821
69. Scahill RI, Schott JM, Stevens JM et al (2002) Mapping the evolution of regional atrophy in Alzheimer's disease: unbiased analysis of fluid-registered serial MRI. *Proc Natl Acad Sci U S A* 99:4703–4707
70. Karas GB, Burton EJ, Rombouts SA et al (2003) A comprehensive study of gray matter loss in patients with Alzheimer's disease using optimized voxel-based morphometry. *NeuroImage* 18:895–907
71. Karas GB, Scheltens P, Rombouts SA et al (2004) Global and local gray matter loss in mild cognitive impairment and Alzheimer's disease. *NeuroImage* 23:708–716
72. Karas G, Sluimer J, Goekoop R et al (2008) Amnesic mild cognitive impairment: structural MR imaging findings predictive of conversion to Alzheimer disease. *AJNR Am J Neuroradiol* 29:944–949
73. Chupin M, Gerardin E, Cuingnet R et al (2009) Fully automatic hippocampus segmentation and classification in Alzheimer's disease and mild cognitive impairment applied on data from ADNI. *Hippocampus* 19:579–587
74. Holland D, Brewer JB, Hagler DJ et al (2009) Subregional neuroanatomical change as a biomarker for Alzheimer's disease. *Proc Natl Acad Sci U S A* 106:20954–20959

75. Smith SM, Jenkinson M, Johansen-Berg H et al (2006) Tract-based spatial statistics: voxelwise analysis of multi-subject diffusion data. *NeuroImage* 31:1487–1505
76. Damoiseaux JS, Smith SM, Witter MP et al (2009) White matter tract integrity in aging and Alzheimer's disease. *Hum Brain Mapp* 30:1051–1059
77. Liu Y, Spulber G, Lehtimäki KK et al (2011) Diffusion tensor imaging and tract-based spatial statistics in Alzheimer's disease and mild cognitive impairment. *Neurobiol Aging* 32(9):1558–1571
78. Teipel SJ, Meindl T, Grinberg L et al (2011) The cholinergic system in mild cognitive impairment and Alzheimer's disease: an in vivo MRI and DTI study. *Hum Brain Mapp* 32(9):1349–1362
79. Teipel SJ, Pogarell O, Meindl T et al (2009) Regional networks underlying interhemispheric connectivity: an EEG and DTI study in healthy ageing and amnesic mild cognitive impairment. *Hum Brain Mapp* 30:2098–2119
80. Arenaza-Urquijo EM, Bosch B, Sala-Llloch R et al (2011) Specific anatomic associations between white matter integrity and cognitive reserve in normal and cognitively impaired elders. *Am J Geriatr Psychiatry* 19:33–42
81. Bosch B, Arenaza-Urquijo EM, Rami L et al (2012) Multiple DTI index analysis in normal aging, amnesic MCI and AD. Relationship with neuropsychological performance. *Neurobiol Aging* 33:61–74
82. Teipel SJ, Meindl T, Wagner M et al (2010) Longitudinal changes in fiber tract integrity in healthy aging and mild cognitive impairment: a DTI follow-up study. *J Alzheimers Dis* 22:507–522
83. Haller S, Nguyen D, Rodriguez C et al (2010) Individual prediction of cognitive decline in mild cognitive impairment using support vector machine-based analysis of diffusion tensor imaging data. *J Alzheimers Dis* 22:315–327
84. O'Dwyer L, Lamberton F, Bokde AL et al (2012) Using support vector machines with multiple indices of diffusion for automated classification of mild cognitive impairment. *PLoS One* 7:e32441
85. Haller S, Lovblad KO, Giannakopoulos P (2011) Principles of classification analyses in mild cognitive impairment (MCI) and Alzheimer disease. *J Alzheimers Dis* 26(Suppl 3):389–394
86. Noble WS (2006) What is a support vector machine? *Nat Biotechnol* 24:1565–1567
87. Plant C, Teipel SJ, Oswald A et al (2010) Automated detection of brain atrophy patterns based on MRI for the prediction of Alzheimer's disease. *NeuroImage* 50:162–174
88. Misra C, Fan Y, Davatzikos C (2009) Baseline and longitudinal patterns of brain atrophy in MCI patients, and their use in prediction of short-term conversion to AD: results from ADNI. *NeuroImage* 44:1415–1422
89. Fan Y, Batmanghelich N, Clark CM et al (2008) Spatial patterns of brain atrophy in MCI patients, identified via high-dimensional pattern classification, predict subsequent cognitive decline. *NeuroImage* 39:1731–1743
90. Haller S, Missonnier P, Herrmann FR et al (2013) Individual classification of mild cognitive impairment subtypes by support vector machine analysis of white matter DTI. *AJNR Am J Neuroradiol* 34:283–291
91. Wee CY, Yap PT, Zhang D et al (2012) Identification of MCI individuals using structural and functional connectivity networks. *NeuroImage* 59:2045–2056
92. Caroli A, Prestia A, Chen K et al (2012) Summary metrics to assess Alzheimer disease-related hypometabolic pattern with 18F-FDG PET: head-to-head comparison. *J Nucl Med* 53:592–600
93. Chen K, Ayutyanont N, Langbaum JB et al (2011) Characterizing Alzheimer's disease using a hypometabolic convergence index. *NeuroImage* 56:52–60
94. Garibotto V, Montandon ML, Viaud CT et al (2013) Regions of interest-based discriminant analysis of DaTSCAN SPECT and FDG-PET for the classification of dementia. *Clin Nucl Med* 38:e112–e117
95. Haense C, Herholz K, Jagust WJ et al (2009) Performance of FDG PET for detection of Alzheimer's disease in two independent multicentre samples (NEST-DD and ADNI). *Dement Geriatr Cogn Disord* 28:259–266
96. Minoshima S, Frey KA, Koeppe RA et al (1995) A diagnostic approach in Alzheimer's disease using three-dimensional stereotactic surface projections of fluorine-18-FDG PET. *J Nucl Med* 36:1238–1248
97. Tomlinson BE, Blessed G, Roth M (1968) Observations on the brains of non-demented old people. *J Neurol Sci* 7:331–356
98. Fotenos AF, Mintun MA, Snyder AZ et al (2008) Brain volume decline in aging: evidence for a relation between socioeconomic status, preclinical Alzheimer disease, and reserve. *Arch Neurol* 65:113–120
99. Garibotto V, Borroni B, Kalbe E et al (2008) Education and occupation as proxies for reserve in aMCI converters and AD: FDG-PET evidence. *Neurology* 71:1342–1349
100. Perneczky R, Haussermann P, Diehl-Schmid J et al (2007) Metabolic correlates of brain reserve in dementia with Lewy bodies: an FDG PET study. *Dement Geriatr Cogn Disord* 23:416–422
101. Premi E, Garibotto V, Gazzina S et al (2013) Beyond cognitive reserve: behavioural reserve hypothesis in frontotemporal dementia. *Behav Brain Res* 245:58–62
102. Roe CM, Mintun MA, Ghoshal N et al (2010) Alzheimer disease identification using amyloid imaging and reserve variables: proof of concept. *Neurology* 75:42–48
103. Vemuri P, Weigand SD, Przybelski SA et al (2011) Cognitive reserve and Alzheimer's disease biomarkers are independent determinants of cognition. *Brain* 134:1479–1492